JOURNAL OF MATERIALS SCIENCE 25 (1990) 3583–3591

Titanium nitride laser-beam surface-alloying treatment on carbon tool steel

T. H. KIM, B. G. SEONG
Department of Metallurgical Engineering, Yonsei University, 134 Shinchondong, Seodaemoongu, Seoul, Korea

In order to improve the wear resistance of tool steel, a study of TiN surface-alloying treatment on 1% carbon steel by irradiation with a CO_2 laser beam was performed. Argon and nitrogen were used as shielding gases, and their effects on the formation of the surface-alloyed layer were investigated. The effect of cobalt additions to the TiN powder on the hardness of the alloyed layer was also investigated. When argon was used as shielding gas, the depth of the alloyed layer was increased compared with the depth when nitrogen was used as a shielding gas. A portion of the TiN decomposed into titanium in the argon environment, the nitrogen apparently being lost as a gas. The structure of the surface-alloyed layer was composed of a ferritic phase without martensitic structure even at high cooling rates. When this layer was annealed at 1000° C for 3 h, part of the titanium precipitated as TiC particles. The hardness of the annealed alloyed layer increased to about 500 Hv. This increase in hardness was accompanied by the appearance of martensite. When nitrogen was used as shielding gas, decomposition of TiN was suppressed and the hardness of the alloyed layer reached 850 Hv. These layers had a martensitic structure. Thus, nitrogen is preferable to argon as a shielding gas if a martensitic structure is desired in this system. When 5% cobalt was added to the TiN powder, the hardness of the alloyed layer increased to 1100 Hv. This increased hardness is caused by stabilization of the martensitic structure caused by an increase in the M_s temperature.

1. Introduction

In surface-alloying treatments of steel by irradiation with laser beams, various alloying elements are applied to the surface of substrate metals by means of vapour deposition, electroplating, ion implantation, plasma spraying or powder coating. These surface-alloying methods can improve wear resistance, corrosion resistance and/or heat resistance of the metal surface while retaining a more ductile core in the substrate metal. In these surface-alloying processes an optimized thickness and composition of the alloyed layer can be obtained. Melting and solidification conditions of the alloyed layer can be controlled by the proper selection of laser power, focusing conditions and scanning speed. The strengthening mechanisms of surface-alloyed layers are the formation of intermetallic compounds, the dispersion of undissolved hard particles, solid solution hardening of alloying elements and martensitic transformations of the alloyed layer by self-quenching [1]. These processes can cause grain refinement in the alloyed layer due to rapid cooling. A number of studies have been published reporting laser surface-alloying treatments with various pure metals and carbides in order to improve the wear resistance of steel [2]. Recently, new laser surface-treating techniques have been reported for nitride, oxide or carbide deposition on surfaces of metals including aluminium, titanium, and zirconium, all having a strong affinity for nitrogen, oxygen and carbon [3–5].

Titanium nitride (TiN) is chemically stable and has a low friction coefficient, a high hardness (2000 kgf mm^{-2}) [6] and a high corrosion resistance. A TiN layer is often applied to the surface of precision tools by a chemical vapour deposition (CVD) or plasma vapour deposition (PVD) process in order to improve their wear resistance. In the CVD process, the processing temperatures are so high that the substrate material is softened. In the PVD process, even though the processing temperatures are low, it takes a much longer time [7]. Laser surface-alloying treatments do not provide such a perfect coating layer on tool steels as the CVD or PVD processes do. However, it takes much less time and the substrate is not affected by heat. Thus laser surfacing is often considered the best process selection to improve wear-resistance for conventional grade tool steels and dies.

This investigation is a basic study to develop a technique for extending the life of a tool steel by applying a TiN laser surface-alloying treatment. Because TiN is easily decomposed at high temperatures, the denitriding phenomena can change the characteristics of the alloyed layer. Therefore, argon and nitrogen were chosen as shielding gases for the laser treatments, and their effects on the formation of the TiN surface-alloyed layer were compared. The effects of cobalt additions to the surface-alloyed layers were investigated.

2. Experimental procedure

The substrate metal used in this work was an annealed-

0022–2461/90 $03.00 + .12

state high carbon tool steel (AISI W1). Its analysed composition (wt %) was: C 1.000, Si 0.246, Mn 0.392, P 0.019, S 0.022, Ni 0.036, Cr 0.050, Al 0.010 and Fe balance. The size of the specimen was 30 mm × 50 mm × 12 mm. The large surfaces were ground flat. The powder sizes used for coating were 1.3 μm for TiN and 1.0 μm for Co, because smaller particle sizes yield better results in laser surface-alloying treatments [8]. The mixing ratios for coatings were 100% TiN and 95% TiN + 5% Co by weight. Both pure TiN powders and powder mixtures were suspended in propyl alcohol. This powder slurry was coated directly on the specimen surfaces to a thickness of 80 μm and then dried.

Each specimen was irradiated with a 1 kW CO_2 laser beam using a scanning speed fixed at 500 mm min^{-1} and a GaAs lens with 12.7 cm. The distance from the laser focal point to the surface of the specimen was set at 5, 10, 15 and 20 mm, and its calculated power density was 6.5×10^5, 1.6×10^5, 7.2×10^4 and 4.0×10^4 W cm^{-2}, respectively. During laser irradiation, argon or nitrogen gas was blown through a nozzle as shielding gas with flow rates of 6, 8, 10 and 12 l min^{-1} by progressively increasing the defocus length ($+d$). In order to investigate the effect of heat treatment on the phase changes and microhardness of alloyed layers, several specimens were annealed at 1000° C for 3 h in 10^{-3} torr vacuum. These specimens were heated to 780° C for 20 min, quenched in 40° C water and then tempered at 170° C for 1 h.

Microstructures and depths of alloyed layers were observed by optical microscopy. Microhardness of the alloyed layer was measured through the thickness dimension with a Vickers microhardness tester with a 100 g load. In order to compare the phase changes in the alloyed layer caused by either the argon or the nitrogen environment during laser irradiation, X-ray diffraction analysis was carried out with a 0.154 06 nm Cu-$K\alpha$ line.

3. Results and discussion

3.1. Microstructure and depth of surface-alloyed layer: effect of shielding gas

When a high-power laser beam irradiates a metal surface, the laser-affected region consists of a laser-melted zone (LMZ) and an unmelted heat-affected zone (HAZ). In the laser-melted zone the metal is heated to a temperature above the melting point and is subsequently resolidified. In the heat-affected zone the metal is heated to a temperature above its transformation temperature but below the solidus. Solid-state transformations in this zone are affected by rapid cooling rates due to self-quenching.

The microstructures of laser beam-affected zones produced when a 95% TiN + 5% Co powder mixture was coated on a specimen and argon was used as shielding gas is seen in Fig. 1. Figs 1a to c show the result of progressively defocusing the beam. As the defocus length increased from 5 mm (6.5×10^5 W cm^{-2}) to 20 mm (4.0×10^4 W cm^{-2}), the depth and width of the laser-affected region increases. However, increasing the defocus length to 20 mm does not result in complete melting of TiN powders. Because the melting point of TiN is 2950° C while that of the substrate is only about 1500° C, the laser-beam power density was insufficient to cause melting and homogeneous distribution of TiN in the alloyed layer. Many undissolved TiN particles are present on the surface layer after irradiation with a 1 kW CO_2 laser at a scanning speed of 500 mm min^{-1} and a defocus length of 20 mm, as seen in Fig. 1c.

Factors related to the distribution of added components in the molten pool are the diffusion of added elements, surface tension gradient changes and the key-hole stirring effect, etc. [9–11]. Of these factors, the violent agitation of the molten pool by the key-hole stirring effect is believed to be the most important for creating a homogeneous distribution of alloying

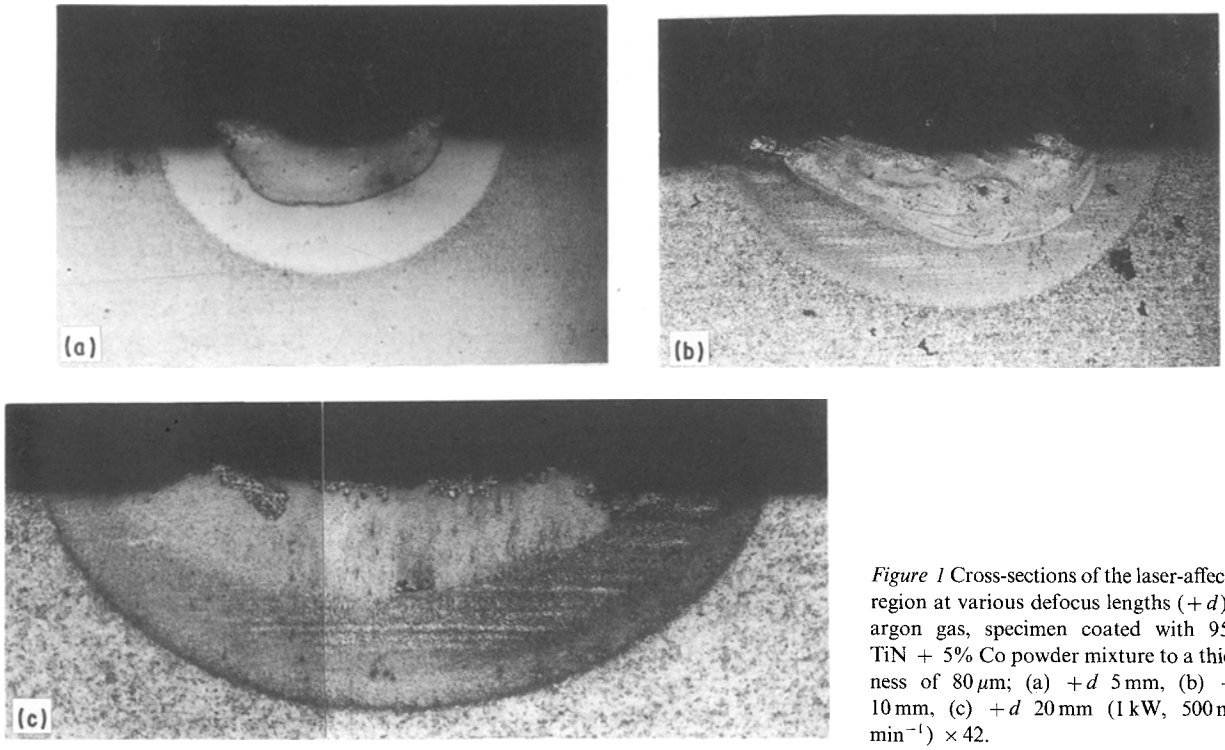

Figure 1 Cross-sections of the laser-affected region at various defocus lengths ($+d$) in argon gas, specimen coated with 95% TiN + 5% Co powder mixture to a thickness of 80 μm; (a) $+d$ 5 mm, (b) $+d$ 10 mm, (c) $+d$ 20 mm (1 kW, 500 mm min^{-1}) × 42.

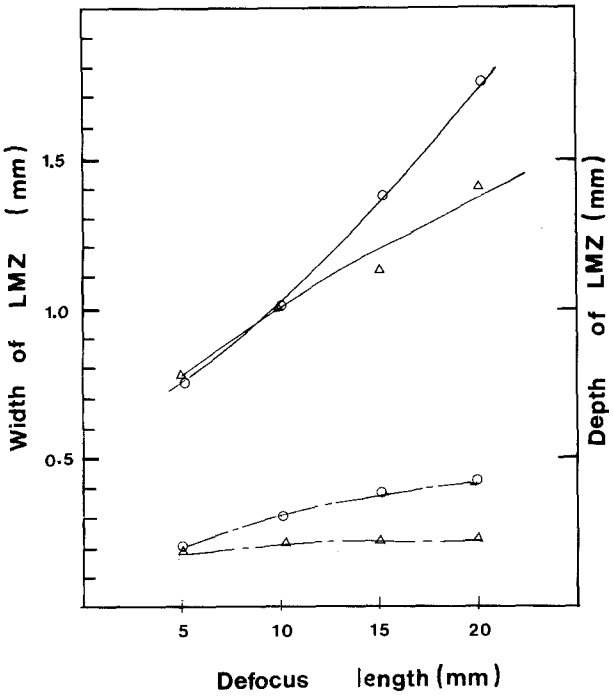

Figure 2 (- - -) Depth and (——) width of laser-melted zone (LMZ) as function of *d*, the defocus length, in both (○) argon and (△) nitrogen gases with 95% TiN + 5% Co (1 kW, 500 mm min^{-1}).

elements in the solidified layer. Longer defocus lengths produce lower laser energy density, decreasing the key-hole penetration. Thus the primary driving force for mixing action becomes weakened and the distribution of solutes becomes heterogeneous in the molten pool.

Fig. 2 illustrates the depth and width of laser-alloyed layers as functions of defocus length for argon and nitrogen. As defocus length was extended, the depth of the alloyed region increased slightly. If the laser beam is focused near the surface, power density increases causing evaporation of the melted surface layer. Evaporated atoms and ejected particles act to shield the incoming laser beam, resulting in a smaller fraction of the beam being absorbed by the liquid. If the defocus length is lengthened, laser power density is reduced and violent evaporation of surface layers is avoided allowing more beam power to reach the surface. Thus the total laser absorption efficiency is enhanced, resulting in an increased depth of the molten layer. Although more substrate layer is melted, TiN particles on surface are not melted completely, as seen in Fig. 1c. In order to obtain a well-developed surface-alloyed layer under these experimental conditions, the optimum defocus length appears to be about 5 mm.

The width of the alloyed layer was increased by extending the defocus length, an observation expected when the focal spot diameter is increased.

Fig. 2 reveals that the depth of the alloyed layer was larger when argon was used as shielding gas. Because the ionization potentials of both argon and nitrogen are high enough as shown in Table I, the plasma formation of either alloying components or shielding gas is not expected even with such a laser power density with a defocusing length of 5 mm. Therefore, the ionization potentials and molecular weights, which have some effects on the removal of plasma, do not seem to be important to explain different behaviours of the molten surface layer. However, the thermal conductivity of nitrogen is larger than that of argon by about 40% as shown in Table I. The thermal energy which is conducted away through the gas is rather higher in a nitrogen environment than that in argon. Also, some laser energy might be consumed by the nitrogen gas due to dissociation of nitrogen molecules into nitrogen atoms. Therefore, it could be expected that the depth of surface-alloyed layer would be reduced in nitrogen gas more than in argon gas.

The microstructures of the zones within the laser-affected region produced with a defocus length of 5 mm in a nitrogen gas with a 95% TiN + 5% Co powder mixture are shown in Fig. 3. The microstructure in (a) represents the upper area of the laser-melted zone. Fine equiaxed grains with less than 5 μm in size are observed. The microstructure in (b) is for a lower area. Grains elongated radially along the direction of heat flow are observed. The white areas represent retained TiN particles which were produced by agglomeration of powders to a size which is too large to be melted in these short times. The microstructure of (c) is taken from the upper area of the heat-affected zone where solid-state transformations occurred by self-quenching. The structure is composed of needle-shaped martensite and bainite. The structures in (d) in a lower area of the heat-affected zone are believed to be bainitic structures.

The microstructure of the central part of a laser-melted regions produced with a defocus length of 5 mm using both argon and nitrogen shielding gases is seen in Fig. 4. The microstructure in (a) shows equiaxed grains under nitrogen shielding gas. The microstructure in (b) produced under argon is a different structure from that in (a), but similar to the structures found in annealed substrate material (c). The difference in structure between (a) and (b) is believed to be due to free titanium produced in the molten pool when argon is used as shielding gas. TiN dissociates into titanium easily at high temperatures under argon gas. Unless there are any restrictions to suppress this dissociation, the concentration of titanium can be increased in the molten layer, the nitrogen apparently being lost as a gas. This titanium will affect the structure of the steel by suppressing austenite formation.

According to the iron–titanium binary phase diagram [12], titanium is a ferrite-forming element in steel as shown in Fig. 5. If the titanium content is above 1.2% in iron, a martensitic transformation cannot take place from a parent austenite phase because the

TABLE I Properties of argon and nitrogen gases

	Ar	N_2
Molecular weight	39.948	28.0134
Specific gravity	1.38	0.9676
Thermal conductivity at 1000 K ($mW\,cm^{-1}\,K^{-1}$)	0.417	0.61
Ionization potential (eV)	15.72	N_2 15.65 N 14.42

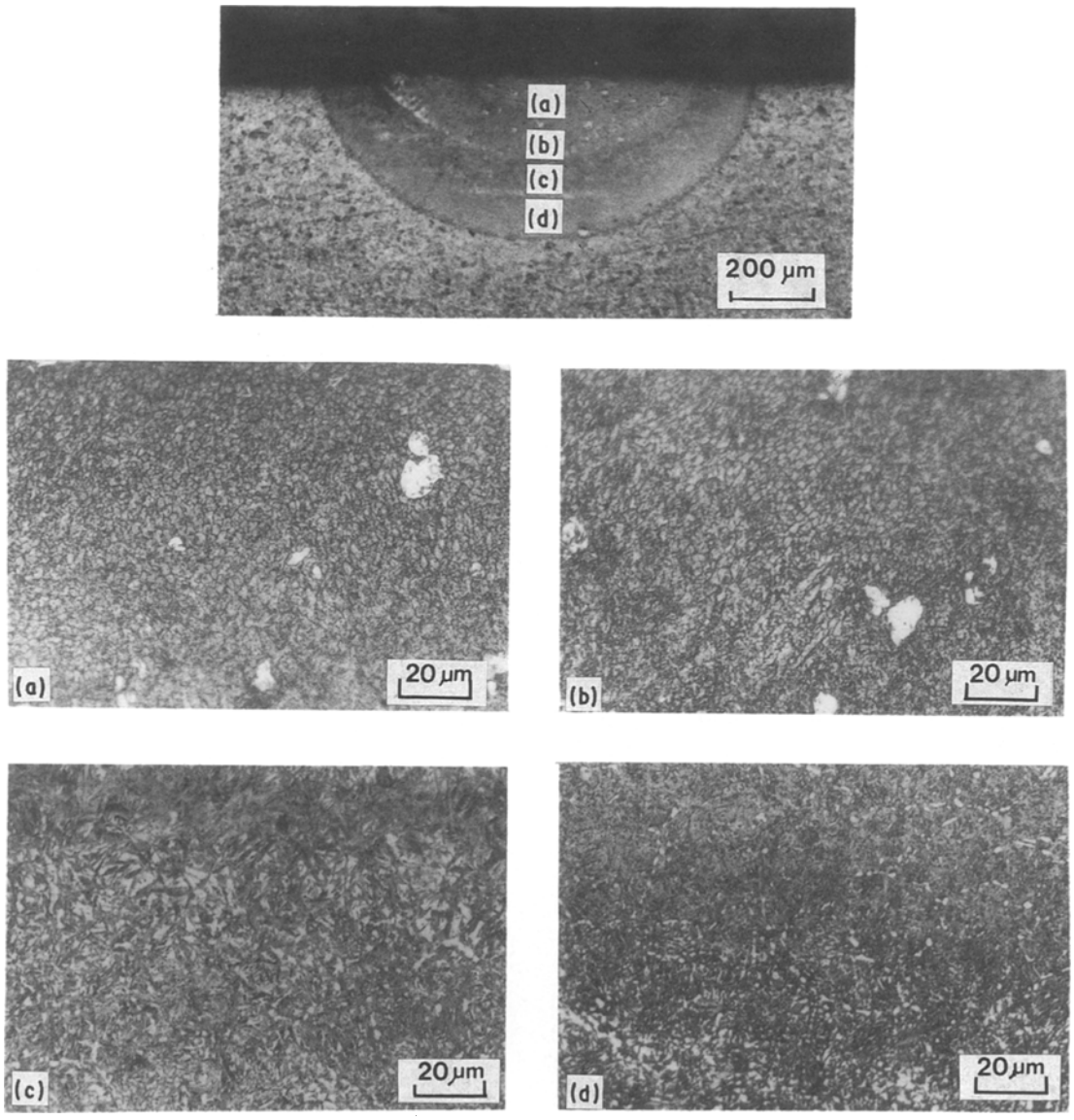

Figure 3 Microstructures of laser-affected zones: 95% TiN + 5% Co powder mixture, defocus length of 5 mm, nitrogen environment, (a) upper LMZ, (b) lower LMZ, (c) upper HAZ, (d) lower HAZ (1 kW, 500 mm min^{-1}).

entire structure is ferritic. Therefore, it is believed that much of the dissociated titanium is dissolved within ferrite grains when using argon. Any remaining titanium segregates on to ferrite grain boundaries, because titanium forms compounds and segregates easily in grain boundaries. When the defocus length was set to more than 15 mm from surface, there were no appreciable differences in the microstructures of molten layers, regardless of the shielding gas used. The reason is believed to be that TiN could not be decomposed at such low laser energy densities even if argon was used as shielding gas.

3.2. X-ray diffraction patterns: effect of titanium

Fig. 6 illustrates the X-ray diffraction patterns for the alloyed layers. Argon and nitrogen were used as shielding gas in (a) and (b), respectively. Here ferrite and TiN peaks were identified in (a), an additional austenite peak was added to those peaks in (b). Because carbon is an austenite-forming element in steel, austenite can be retained in high carbon steel after rapid cooling. In the case of 1% C steel the austenite can reach about 15% [13]. Nitrogen also acts as an austenite former in steel.

The addition of titanium in iron gives a gamma-closed phase diagram as seen in Fig. 5. When titanium reaches about 0.7% in iron, a ferritic phase appears in austenite at 1150° C. The austenite phase disappears completely when it exceeds 1.2% in iron. Therefore, it is expected that a martensitic transformation cannot occur in iron when the titanium content is more than 1.2% even if its cooling rate is very rapid. However, the amount of titanium should be much higher than this value in high carbon steel in order to get rid of the austenite in structure. Because carbon is an austenite-forming element in steel as mentioned, it should be compensated by the equivalent amount of titanium, which is a ferrite-forming element, to avoid the effect of carbon in ferrite–austenite transformation. Therefore, it can be reasoned that much of TiN decomposes in titanium when argon is used as a shielding gas. The absence of an austenite peak in Fig. 6a means that very little, if any, austenite was retained in the alloyed

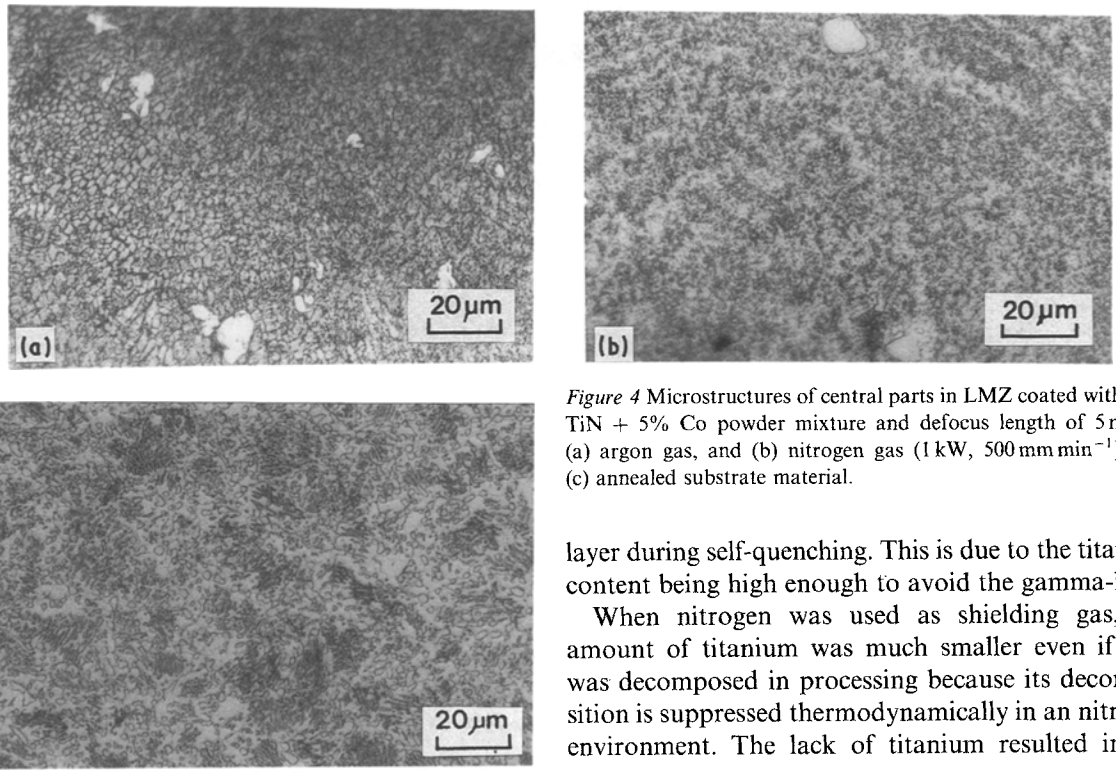

Figure 4 Microstructures of central parts in LMZ coated with 95% TiN + 5% Co powder mixture and defocus length of 5 mm in (a) argon gas, and (b) nitrogen gas (1 kW, 500 mm min^{-1}), and (c) annealed substrate material.

layer during self-quenching. This is due to the titanium content being high enough to avoid the gamma-loop.

When nitrogen was used as shielding gas, the amount of titanium was much smaller even if TiN was decomposed in processing because its decomposition is suppressed thermodynamically in an nitrogen environment. The lack of titanium resulted in the

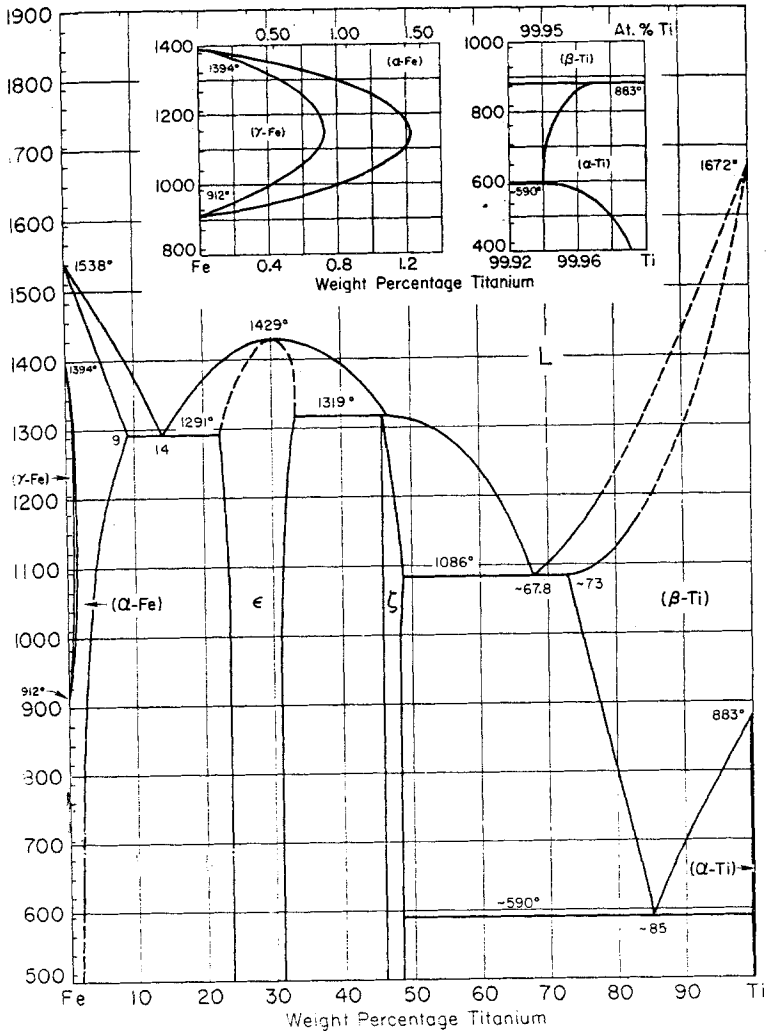

Figure 5 Phase diagram of the titanium–iron system [12].

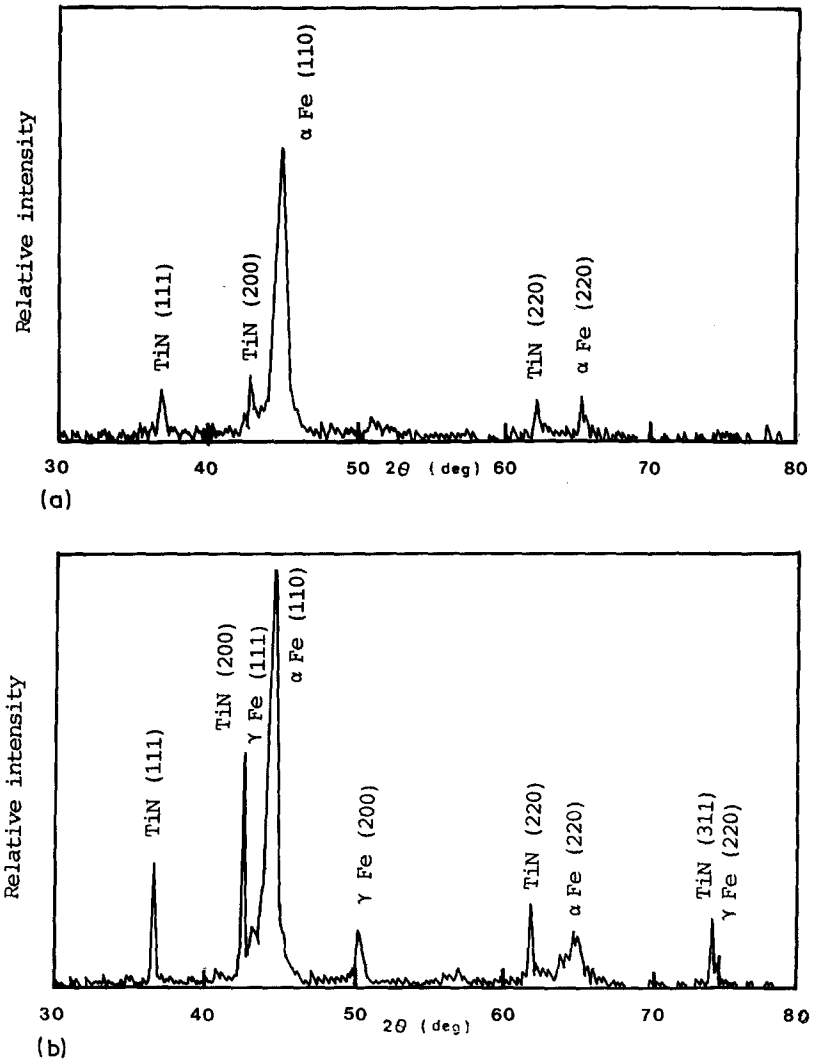

Figure 6 X-ray diffraction patterns of LMZ coated with 95% TiN + 5% Co powder mixture and defocus length of 5 mm in (a) argon gas, and (b) nitrogen gas, (1 kW, 500 mm min^{-1}, 0.154 06 nm Cu-$K\alpha$ line).

presence of retained austenite after the martensitic transformation of the surface layer.

Although most alloying elements decrease the critical cooling rate for a martensitic transformation in steel, titanium increases this value very rapidly when it is added in amounts more than 0.2% as shown in Fig. 7 [14]. If titanium is present in steel, a more rapid cooling rate is required to cause martensitic transformation of steel and to retain less austenite in the structure. Therefore, an increase in the critical cooling rate due to decomposed titanium content in steel would result in a further increase of retained austenite in the alloyed layer under an argon environment.

3.3. Microhardness of the surface-alloyed layer: effect of cobalt addition

In order to investigate enhanced wear resistance of the alloyed layer, the microhardness was measured in the laser-affected region. Fig. 8 illustrates the distribution of hardness in an alloyed layer produced with a TiN powder coating under argon gas as a function of defocus length and distance along the depth from the surface. In the case of a defocus length of 5 mm, the hardness of the alloyed layer was low, around 300 Hv. The substrate structure contained spherodized carbides and had a hardness of 250 Hv. The similarity in hardnesses agrees with the similarity of their microstructures as shown in Fig. 4. This result supports the fact that much TiN was decomposed into titanium during processing under an argon environment and the composition of the alloyed layer is in the ferrite region around 1150° C (see Fig. 5). Thus a martensitic transformation could not occur in the alloyed layer when it was cooled rapidly from melting point to room temperature, and the hardness could not be very high.

In the cases of processing with defocus lengths of 10 and 15 mm, the hardness of the alloyed layer increased to 500 to 700 Hv. The reason for this increase was believed to be that the laser power density was less than that obtained at 5 mm, and thus the

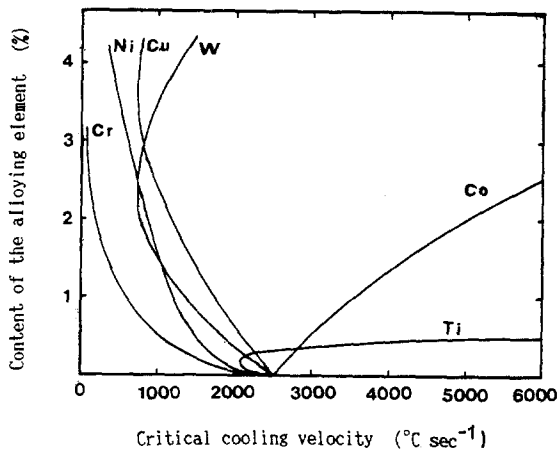

Figure 7 The effect of various alloying elements on the critical cooling rate in the martensitic transformation of steel [14].

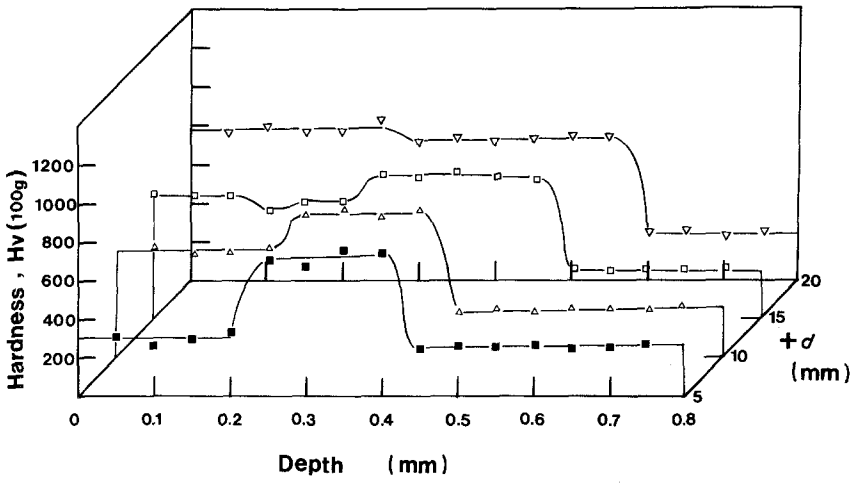

Figure 8 Hardness of the laser-affected regions as functions of the defocus length ($+d$) and the depth from surface coated with TiN powder in argon gas (1 kW, 500 mm min^{-1}).

decomposition of TiN was reduced to less than 1.2% Ti. But this alloyed layer passed through the austenite–ferrite region in the Fe–Ti phase diagram during the cooling cycle, and austenite transformed to martensite due to self-quenching. Therefore, a hardened layer which consisted of ferrite and martensite was obtained from the structure. If the defocus length was increased to 20 mm, the laser power density was much less and the decomposition of TiN was suppressed. Therefore, this alloyed layer could pass through the austenitic region and could be transformed to martensite during rapid cooling, yielding a hardness of 800 Hv. The structure of the heat-affected zone was martensite with some bainite, and its hardness was 750 to 800 Hv.

Fig. 9 illustrates the distribution of hardness in the alloyed layer when a 95% TiN + 5% Co powder coating was processed under argon gas. The amount of 5% Co in the powder mixture is equivalent to less than 1% Co in the alloyed layer, because the thickness of the alloyed layer is several times larger than that of the coating layer. Cobalt increases the M_s temperature of steel during martensitic transformations [15]. A small addition of cobalt can accelerate the martensitic transformation of the alloyed layer by elevating the M_s temperature, decreasing the amount of retained austenite. However, too much cobalt in steel is undesirable to obtain high hardness by martensitic transformation, because cobalt is an austenite stabilizing element which also increases the critical cooling rate for martensitic transformation as shown in Fig. 7. According to previous studies on surface alloying of carbon tool steel with high melting temperature materials (tungsten, tungsten carbide and titanium carbide), less than 10% cobalt in the powder mixtures produced better results [16–18].

When argon was used as shielding gas, the alloyed layer was not transformed to martensite as explained in Section 3.1. Therefore, the cobalt addition in the coating powder did not affect the hardness as shown in Fig. 9.

Fig. 10 illustrates the distribution of hardness in an alloyed layer produced with a TiN powder coating under nitrogen gas. Here, in the case of processing with a defocus length of 5 mm, the hardness of the alloyed layer was 850 Hv, in contrast with 300 Hv obtained under argon gas (see Fig. 8). This result again indicates that the decomposition of TiN is suppressed under a nitrogen environment to give less than 1.2% Ti in the molten layer. Thus a martensitic transformation of the alloyed layer was possible. Fig. 11 illustrates the hardness of an alloyed layer with 95% TiN + 5% Co powder under nitrogen gas. With a defocus length of 5 mm the hardness of the alloyed layer was 1100 Hv, which was much higher than any value found in Fig. 10. The increase in hardness is believed primarily due to the effect of the cobalt addition in the alloyed layer. As the focus length increased the hardness of the alloyed layer tended to decrease slightly. The laser beam power density decreased and complete melting and dissolution of

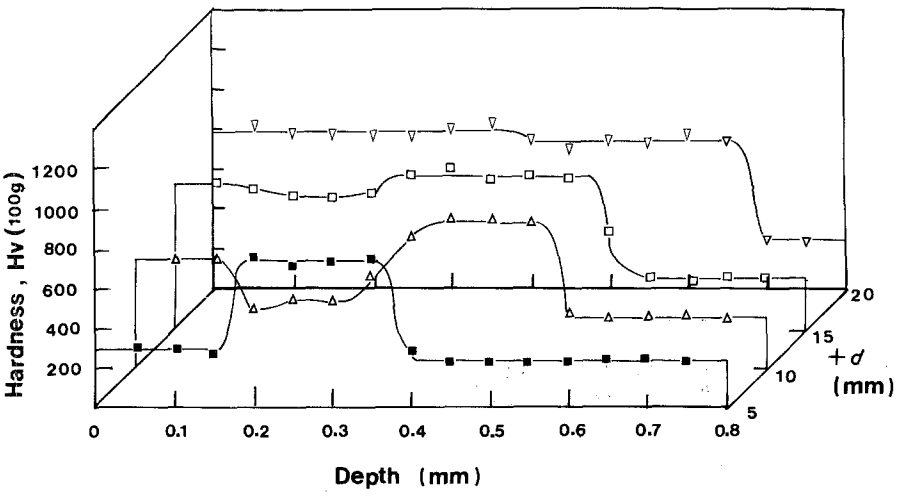

Figure 9 Hardness of the laser-affected regions as functions of the defocus length ($+d$) and the depth from surface coated with 95% TiN + 5% Co powder mixture in argon gas (1 kW, 500 mm min^{-1}).

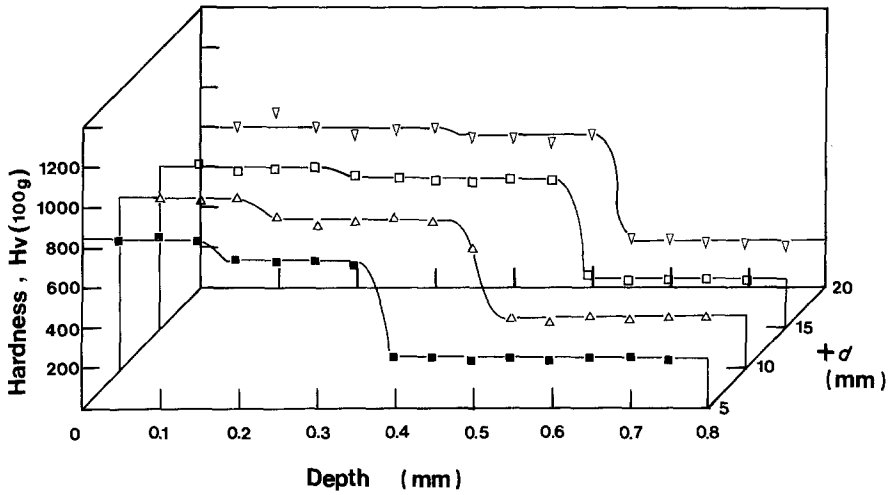

Figure 10 Hardness of the laser-affected regions as functions of the defocus length ($+d$) and the depth from the surface coated with TiN powder in nitrogen gas (1 kW, 500 mm min^{-1}).

TiN into the melted region was incomplete. Thus the concentration of distributed TiN particles was reduced. The alloyed layers have a slightly higher hardness compared with heat-affected regions in all cases. This is due to the homogeneous distribution of TiN particles and the grain refinement in the alloyed region.

Fig. 12 illustrates the effect of heat treatment on hardness of the laser-affected region which was produced under an argon environment. Heat treatment increased the hardness in the alloyed layer by about 500 Hv as shown in (a). Because the decomposition of TiN into titanium caused the suppression of austenite, a martensitic structure was not produced under argon gas. However, titanium is a much stronger carbide former than iron in carbon steel. Thus most isolated titanium would precipitate as TiC by combining with carbon from Fe_3C during the heat treatment of the alloyed layer at 1000° C for 3 h. The dissociated titanium in the alloyed layer is thus reduced, causing the formation of austenite and the resulting martensitic transformation during quenching after the annealing treatment. While the depletion of titanium in the alloyed layer has strong influences on the transformation behaviours and structures, precipitated TiC particles can further enhance hardness in the alloyed layer.

The hardness distribution in an alloyed layer produced using 5% cobalt in the powder mixture is seen in Fig. 12b. The hardness value was higher than that in (a). Again the increased hardness can be attributable to enhanced martensitic transformation in the alloyed layer with cobalt additions. When 1% C steel is quenched rapidly, its hardness reaches 870 Hv [19]. The hardness of the heat-affected zone after heat treatment (see Fig. 12b) is about 750 Hv, which is lower than the as-quenched value by about 120 Hv. This is because the structure was softened during the tempering process performed after quenching.

Considering the fact that the hardness of a bainitic structure is close to that of tempered martensite, it is speculated that the martensite-like structure in the laser-alloyed zone in Fig. 12a is primarily bainitic structure.

From this work it is found that the laser power density, the shielding gas and the addition of alloying elements have significant effects on the solid-state transformations and structures of an alloyed layer in TiN laser surface-alloying process of carbon tool steel.

4. Conclusions

When a TiN surface-alloyed layer was produced on carbon tool steel using a CO_2 laser beam, the depth of the alloyed layer was increased if argon was used as shielding gas over that produced when nitrogen was used.

With argon, a portion of the TiN was decomposed into titanium during laser processing, and the resulting dissolved titanium caused a suppression of austenite during rapid cooling. Thus a martensitic structure could not be obtained in a surface-alloyed layer using argon as a shielding gas. If this layer was annealed at

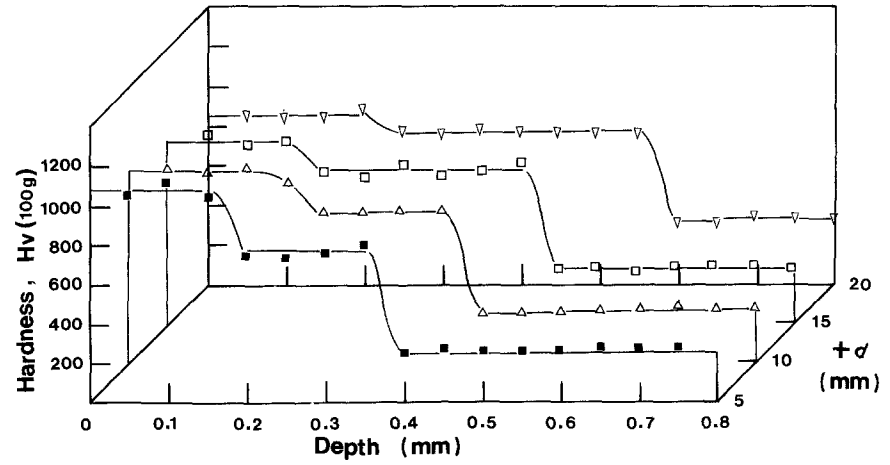

Figure 11 Hardness of the laser-affected regions as functions of the defocus length ($+d$) and the depth from the surface coated with 95% TiN + 5% Co powder mixture in nitrogen gas (1 kW, 500 mm min^{-1}).

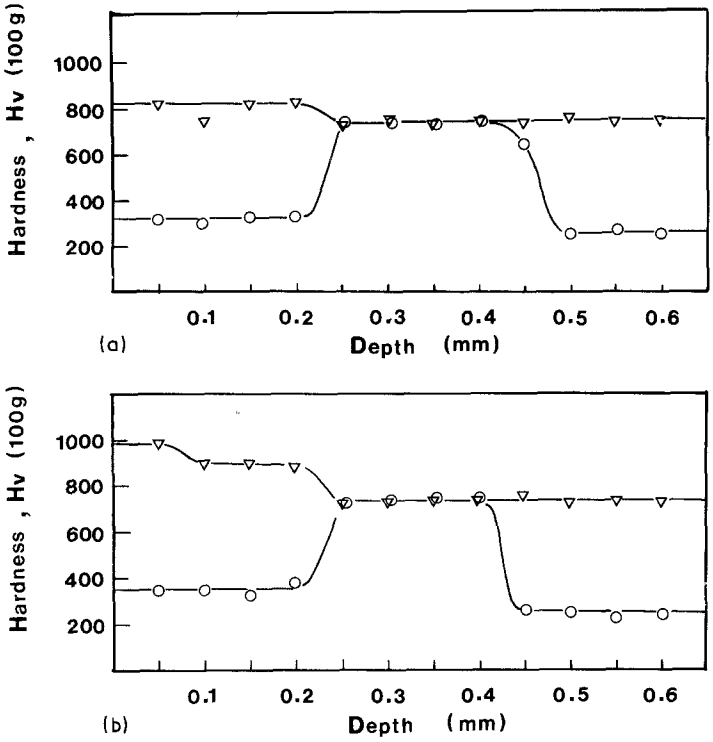

Figure 12 Effect of the heat treatment on the hardness of laser-melted zone obtained in argon gas, (a) TiN pwoder coating, (b) 95% TiN + 5% Co powder mixture coating (1 kW, 500 mm min^{-1}). (▽) Heat-treated, (○) normal.

1000° C for 3 h, dissolved titanium was precipitated into TiC. The austenite transformation was no longer suppressed, and thus a martensitic structure could be obtained during rapid cooling.

When nitrogen was used as shielding gas, decomposition of TiN was avoided in the alloyed region during laser processing and a martensitic structure was obtained by self-quenching. Therefore, nitrogen is preferable to argon as a shielding gas in order to produce an alloyed layer with a martensitic structure.

A homogeneous alloyed layer with a thickness of abut 200 μm was obtained by using a power of 1 kW and scanning speed of 500 mm min^{-1}.

If 5% cobalt was added to the TiN powder used as a coating material, a martensitic transformation was enhanced by the elevation of the M_s temperature. The hardness reached 1100 Hv in this alloyed region.

Acknowledgements

This work was supported by the Korean Ministry of Education. Dr Kim, visiting professor, Department of Welding Engineering, Ohio State University, USA, thanks Professor C. E. Albright for proof reading the paper.

References

1. T. H. KIM, M. G. SUK, P. S. PARK and K. H. SUH, in "World Lasers Almanac 1988" (Sprechsaal, Coburg, West Germany, 1988) p. 35.
2. C. W. DRAPER and C. A. EWING, *J. Mater. Sci.* **19** (1984) 3815.
3. H. W. BERGMAN, S. LEE and T. BELL, in Proceedings of the 3rd International Conference on Lasers in Manufacturing, Paris, June 1986, edited by A. Quenzer (IFS, Bedford, 1986) p. 221.
4. I. URSU, I. N. MIHAILESU and A. N. PROKHOROV, *J. Phys. D, Appl. Phys.* **18** (1987) 2547.
5. K. KAWACHI, N. MORISHIGE and S. SETO, in Proceedings of LAMP '87, Laser Advanced Materials Processing – Science and Applications, Osaka, May 1987 (High Temperature Society of Japan, Osaka University, 1987) p. 471.
6. J. E. SUNDGREN, *Thin Solid Films* **21** (1985) 128.
7. A. E. ANDERSON, *Met. Prog.* August (1985) 41.
8. T. H. KIM and Y. K. KIM, *J. Korean Inst. Metals* **23** (1985) 1241.
9. L. S. WEINMAN and J. N. DEVAULT, in Proceedings of Laser-Solid Interactions and Laser Processing – 1978, Boston, edited by S. D. Ferris, H. T. Leamy and J. M. Poate (1978) p. 239.
10. T. R. ANTHONY and H. E. CLINE, *J. Appl. Phys.* **48** (1977) 3888.
11. M. BASS, in "Laser Materials Processing" (North-Holland, Amsterdam, 1983) p. 119.
12. "Metals Handbook", Vol. 8, 8th Edn (ASM, 1973) p. 307.
13. C. S. CHOI and H. C. YOO, *J. Korean Inst. Metals* **15** (1977) 550.
14. H. Y. YANG and S. Y. KIM, in "Metallic Materials" (Moon Un Dang, Seoul, 1984) p. 237 (in Korean).
15. F. B. PICKERING, in "'Physical Metallurgy and the Design of Steels" (Applied Science, London, 1978) p. 185.
16. T. H. KIM and M. G. SUK, *J. Korean Inst. Metals* **25** (1987) 307.
17. T. H. KIM and B. S. PARK, *ibid.* **25** (1987) 209.
18. T. H. KIM and K. H. SUH, *ibid.* **26** (1988) 800.
19. G. ROBERTS and R. CRAY, in "Tool Steels", 4th Edn (ASM, Metals Park, 1980) p. 300.

Received 6 April
and accepted 28 September 1989